Understanding the High Activity of a Nanostructured Catalyst Obtained by a Deposit of Pd on Ni: First Principle Calculations

J.-S. Filhol,[†,‡,||] D. Simon,[†,§] and P. Sautet*,[†,‡]

Contribution from the Laboratoire de Chimie, École Normale Supérieure de Lyon and CNRS, 46 allée d'Italie, 69364 Lyon Cedex 07, France, Institut de Recherches sur la Catalyse, CNRS, 2 avenue A. Einstein, 69626 Villeurbanne Cedex, France, and Laboratoire de Spectrométrie Ionique et Moléculaire, Université de Lyon I and CNRS, 69622 Villeurbanne Cedex, France

Received August 27, 2003; E-mail: sautet@ens-lyon.fr

Abstract: The catalytic activity of a 4 monolayer deposit of Pd on a Ni(110) surface toward the hydrogenation of ethylene is investigated by using gradient-corrected periodic density functional calculations. The Pd/Ni(110) surface is strongly nanostructured, due to the anisotropic stress induced by the Ni(110) substrate on the Pd layer. A kinetic analysis, based on the investigation of the optimal reaction pathway for the hydrogenation of ethylene to ethane, is presented, allowing a comparison between Pd/Ni(110) and pure Pd(110) surfaces. The calculated activation energies allow one to reproduce the experimental result, which shows that the Pd/Ni(110) surface is about 30 times more active than the pure Pd(110) surface. This marked increase of the catalytic activity is a consequence of the specific nanostructure of the Pd/Ni(110) surface. By examining the structure of the adsorbed species and of the transition states and by analyzing the electronic properties, we show that this rate increase can be associated to the fact that the ethylene adsorption energy in the first hydrogenation step and the ethyl-hydrogen coadsorption energy in the second step are both much lower on Pd/Ni(110) than on pure Pd(110).

Introduction

Catalysts are used in most industrial processes to increase the rate of numerous reactions that even sometimes would not occur at the human time scale. They allow the use of milder chemical reaction conditions and lead to a huge saving in the fabrication costs. Renewed research to find more effective catalysts is then fundamental to improve efficiency and cut the costs. At the same time, the rapid development of nanoscience and the ability to synthesize new nanostructured chemical objects allows a better control of matter organization at the nanoscale.[1−3] This opens the way to the design of new catalysts from the controlled fabrication of nanometer scale structures.[4−6] Two directions are emerging: the creation of metal clusters with controllable sizes and shapes[7] or the spontaneous formation of organized nanopatterns at surfaces. The driving force for the formation of well-controlled nanoscale structures on a metal surface can be the stress induced when a metal is deposited on another metal with a different lattice parameter. The periodic array of dislocations which forms by the deposit of a bilayer of Cu on a Pt(111) surface was, for example, used as a template to form highly ordered ensembles of nanostructures by further deposition of iron or silver.[8] The case we will focus on in this paper is a deposit of Pd on a Ni(110) surface, which shows two specific properties. It gives a large enhancement of the catalytic activity for the hydrogenation of butadiene and alkenes, the maximum amplification, by 2 orders of magnitude in comparison to the already very active Ni surface, being obtained for a deposit of four monolayers.[9,10] Moreover, such a deposit presents a clear nanostructure with a large anisotropy of the surface pattern: the periodicity is 11 times the lattice constant in the dense row [1$\bar{1}$0] direction, but only 2 times the lattice constant in the perpendicular direction. This surface reconstruction is clearly induced by the strain at the Pd/Ni interface and the related stress field in the deposit.[11,12] The relation between the enhanced catalytic activity and the nanostructured surface is, however, not clearly understood and is the focus of this theoretical study. Additional evidence for nanometer-size effects

---

† Laboratoire de Chimie, CNRS.
‡ Institut de Recherches sur la Catalyse, CNRS.
§ Laboratoire de Spectrométrie Ionique et Moléculaire, Université de Lyon I and CNRS.
|| Present address: Laboratoire de Structure et Dynamique des Systèmes Moléculaires et Solides, Université Montpellier II and CNRS, place E. Bataillon, 34095 Montpellier Cedex 5, France.

(1) Lee, J.; Kim, H.; Kahng, S.-J.; Kim, G.; Son, Y.-W.; Ihm, J.; Kato, H.; Wang, Z. W.; Okazaki, T.; Shinohara, H.; Kuk, Y. *Nature* **2002**, *415*, 1005.
(2) Heinrich, B. *Can. J. Phys.* **2000**, *78*, 161.
(3) Ibn-Elhaj, M.; Schadt, M. *Nature* **2001**, *410*, 796.
(4) Bell, A. T. *Science* **2003**, *299*, 1688.
(5) Egeberg, R.; Chorkendorff, I. *Catal. Lett.* **2001**, *77*, 207.
(6) Bertolini, J.-C. *Appl. Catal., A* **2000**, *191*, 15.
(7) Maye, M. M.; Luo, J.; Lim, I. S.; Han, H.; Kariuki, N. N.; Rabinovitch, D.; Liu, T.; Zhong, C. J. *J. Am. Chem. Soc.* **2003**, *125*, 9906.

(8) Brune, H.; Giovanni, M.; Bromann, K.; Kern, K. *Nature* **1998**, *394*, 451.
(9) Porte, L.; Phaner-Goutorbe, M.; Guigner, J.; Bertolini, J.-C. *Surf. Sci.* **1999**, *424*, 262.
(10) Abel, M.; Robach, Y.; Bertolini, J.-C.; Porte, L. *Surf. Sci.* **2000**, *454−456*, 1.
(11) Besenbacher, F.; Pleth Nielsen, L.; Sprunger, P. T. In *The Chemical Physics of Solid Surfaces*; King, D. A., Woodruff, D. P., Eds.; Elsevier: Amsterdam, 1997; Vol. 8.
(12) Pohl, K.; Bartelt, M.; de la Figuera, J.; Bartelt, N.; Hrbek, J.; Hwang, R. *Nature* **1999**, *397*, 238.

in surface reactivity has been reported in the case of faceted monolayer films of Pt or Pd on a W(111) surface.[13]
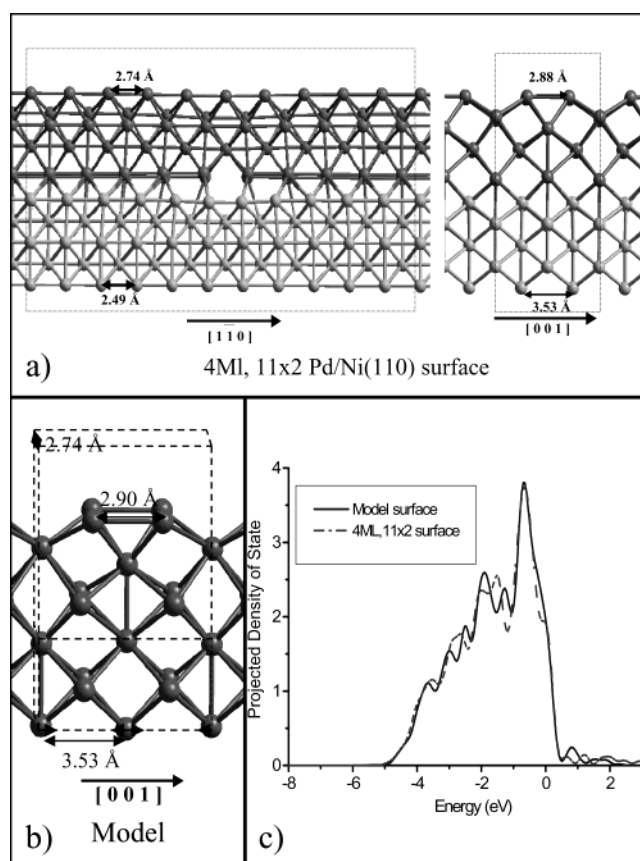
In contrast to usual surfaces, the structures of the deposits of Pd on Ni were unknown and complex, showing in the case of four layers of Pd an 11 × 2 surface reconstruction. These surface structures needed to be fully characterized and understood because at the nanoscale the local arrangement of atoms is expected to be crucial for the chemical reactivity.

The first step was then to determine the structure and phase diagram[14,15] of these deposits from first principle calculations. These were successfully compared to the experimental[16] results, in particular for the 4 monolayer (ML) deposits that were found to be the most catalytically active. The second and final step of this study is presented in this Article, where we focus on the pathway and kinetics for the catalytic hydrogenation of ethylene on this nanostructured deposit surface, to understand the origin of the activity enhancement. First, a simplified model of the complex deposit is built, keeping all critical structural and electronic features, to allow a first principle exploration of reaction pathways and an accurate determination of transition states. We then focus on the hydrogenation of ethylene on this model deposit using the Pd(110) surface as a reference.

The 11 × 2 surface nanopattern originates from the release of the compressive stress of the Pd layers at the interface, because the Pd atomic radius is 10% larger than that of Ni. This reconstruction is driven by a dual mechanism, depending on the directions on the (110) surface (Figure 1a). Along the dense row [1$\bar{1}$0] direction, a periodic array of dislocations forms at the interface, which restores, at the surface, a bulklike Pd−Pd distance. More precisely, an atomic vacancy is formed at the interface every 10 Pd atoms, allowing one to position in the deposit 10 Pd atoms in the space where 11 Ni are found in the substrate, hence relaxing the stress in the Pd deposit layers. In the perpendicular [001] direction (Figure 1a), the stress induced by the Ni substrate creates a strongly distorted surface structure, with rows shifted by 0.3 Å, associated with a Pd−Pd interaction between two paired rows, at a distance of 2.88 Å.[16] Such a pairing-buckling reconstruction does not exist on the pure Pd(110) surface. A completely new coordination of surface Pd atoms hence appears on the Pd/Ni(110) deposit with the formation of square arrangements. This specific self-organized superstructure could be the key point of the exaltation of the catalytic activity of the surface. The identification of the reaction pathways on the example of ethylene hydrogenation will clarify the relationship between the nanostructure and the reactivity.

Computational Methods and Systems

The calculations were performed using the plane-wave density functional theory (DFT) code Vasp[17,18] with Vanderbilt ultrasoft pseudopotentials.[19,20] The exchange-correlation energy and potential are described by the generalized gradient approximation (Perdew−Wang 91[21]). The surfaces are represented by periodic slabs using at least a vacuum of 12 Å between them.

(13) Madey, T.; Pelhos, K.; Wu, Q.; Barnes, R.; Ermanoski, I.; Chen, W.; Kolodziej, J.; Rowe, J. *Proc. Natl. Acad. Sci. U.S.A.* **2002**, *99*, 6503.
(14) Filhol, J.-S.; Simon, D.; Sautet, P. *Phys. Rev. B* **2001**, *64*, 85412.
(15) Filhol, J.-S.; Simon, D.; Sautet, P. *Surf. Sci.* **2001**, *472*, L139.
(16) Filhol, J.-S.; Saint-Lager, M.-C.; Santis, M. D.; Dolle, P.; Simon, D.; Baudoing-Savois, R.; Bertolini, J.; Sautet, P. *Phys. Rev. Lett.* **2002**, *89*, 146106.
(17) Kresse, G.; Hafner, J. *Phys. Rev. B* **1994**, *49*, 14251.
(18) Kresse, G.; Furthmüller, J. *Comput. Mater. Sci.* **1996**, *6*, 15.
(19) Vanderbilt, D. *Phys. Rev. B* **1990**, *41*, 7892.
(20) Kresse, G.; Hafner, J. *J. Phys.: Condens. Matter* **1994**, *6*, 8245.

Figure 1. (a) Structure of a 4 ML, 11 × 2 Pd/Ni(110) deposit in two different directions. The main geometric elements are presented. The unit cell is indicated by a dashed line. (b) Structure of the Pd 2 × 2 model for the Pd/Ni 11 × 2 deposit. Some of the geometric elements are presented. The unit cell is indicated with a dashed line. (c) Local density of states projected on a surface Pd atom of the model structure, whose unit cell is presented in (b) (line) and of the 11 × 2 realistic structure presented in (a) (dashed line). The energy reference is the Fermi level.

The 11 × 2 experimental nanostructure of the Pd deposition on Ni necessitates 190 metal atoms in the unit cell and at least 1900 electrons to be completely described[16] (see Figure 1a). Although such a complex system can be simulated with the considered approach, it is not possible to carry a full reaction path search with such a large unit cell. Moreover, only the uppermost Pd atoms are expected to have an important impact on the surface reactivity because, for this thick deposit, the direct chemical influence of the deep Ni atoms is supposed to be weak: the main effect of the Ni substrate is to impose an epitaxial strain on the Pd layer at the interface.

Furthermore, the surface Pd structure is rather homogeneous in the dense row direction. A simplified model system can be constructed by applying to a Pd surface the residual strain observed in the real Pd on Ni deposit. Hence, a slab of Pd is constructed, made of 6 layers, the top 3 layers being allowed to relax and the lower 3 layers remaining frozen in a geometry identical to the pseudo epitaxial position found in the Pd−Ni interface of the true Pd/Ni(110) 11 × 2 unit cell. The model system consists of a 2 × 2 Pd(110) unit cell, but the cell parameters are constrained to the average Pd−Pd distance observed in the Pd on Ni deposit, giving box sizes of 5.48 Å in the [1$\bar{1}$0] direction and 7.06 Å in the [001] direction (Figure 1b). This corresponds to a compressive strain of 2% and 10.9% in each direction, respectively. This differs from the (1 × 1) epitaxial model, which would apply a strain of 10.9% for each direction, and takes into account the structural relaxation observed in the row direction for the real deposit.

(21) Perdew, J. P.; Chevary, J. A.; Vosko, S. H.; Jackson, K. A.; Pederson, M. R. *Phys. Rev. B* **1992**, *46*, 6671.

The key point, which validates this simplified constrained Pd model of the Pd/Ni deposit, is that, with this constraint applied in the 3 bottom layers of the slab, the surface does not adopt the usual 1×1 geometry, but reconstructs with a geometry which is completely similar to that of the peculiar deposit (Figure 1b) with the striking row pairing process (with a distance between paired rows of 2.90 Å, very close to the 2.88 Å in the true deposit) and also an identical buckling in the second layer. In addition, the surface electronic structure of this strain-induced reconstruction of Pd(110) matches very well the one calculated for the full 11×2 Pd on Ni deposit (Figure 1c). The unique local environment of the surface Pd atoms in the Pd/Ni(110) nanostructured deposit is hence perfectly taken into account in the model surface, as demonstrated by the nearly identical electronic properties: this model should reproduce very closely the reactivity of the experimental Pd/Ni(110) system. The surface Pd structure of the 11×2 reconstruction can then be seen as an hybrid (110)−(100) Pd surface that is only stable because of the epitaxial strain imposed by the Ni(110) substrate. The creation of the quasi-square surface sites in the nanostructure should induce a completely new range of catalytic behaviors. It should be underlined here that such a pairing row reconstruction is not stable on a normal Pd(110) surface and is stabilized in the deposit, or in its simple 2×2 model, by the natural or imposed interfacial strain.

For this 2×2 Pd(110) slab, a Monkhorst−Pack mesh of $5 \times 3 \times 1$ k-points and a cutoff energy of 287 eV were used. The optimization is achieved by using analytical calculations of Hellmann−Feynman forces acting on the atoms of the unit cell.

The molecular coverage for ethene (our model alkene) on the (2×2) surface is 0.25 ML. Such a coverage can be easily reached for ethene adsorption on metal surfaces. We have, however, checked the convergence of the calculated energy for ethene adsorption and coadsorption with hydrogen by enlarging the unit cell to 4×2 (0.125 ML). The variation of binding energy is less than 2 kJ mol^{-1}, hence showing that the interaction between periodic images in the 2×2 unit cell is small. Furthermore, the purpose of this study is not to reach absolute binding energies and barriers but to compare similar systems: the strain-induced reconstruction of Pd(110) (as a model for the Pd/Ni deposit) and the normal Pd(110) surface. Hence, from cancellation of errors, the variation of activation barriers and the ratio of the calculated rate constants (i.e., the activity ratio) are far more precise than the absolute values. This should allow us to compute proper variation of the catalytic activity of the Pd/Ni(110) in comparison to the Pd(110) surface.

The transition states were reached by an initial crude search, refined by an iterative estimation and inversion of the Hessian matrix until convergence toward a transition state. The validity of the obtained transition state was checked by a full vibrational calculation achieved by a complete calculation of the Hessian matrix followed by a diagonalization procedure to obtain the eigenmodes.[22] The states should only present one negative force constant, the others being positive. We then checked that the eigenvector associated with the negative force constant was related to the considered reaction pathway. This procedure allows one to obtain accurate transition states and activation barriers.

Results

In this section, the "Pd/Ni model deposit" will refer to the stained and reconstructed Pd slab, as explained above. On the Pd/Ni model deposit, as well as the pure Pd(110) surface, the most stable coadsorption state corresponds to an ethylene molecule in a bridge site, with hydrogen atoms in pseudo-three-fold sites inside the grooves.[23] A short distance repulsive lateral interaction is present so that the H atoms tend to move the largest distance from the molecule that is allowed from the unit cell.

One important difference for the strained deposit is that the coadsorption energy for this initial state is significantly reduced (by 16 kJ mol^{-1}), as compared to the pure Pd(110) surface. This is mainly related to a weaker Pd−ethylene bond on the deposit.

Reaction pathways for hydrogenation have been exhaustively explored, and three low energy profiles have been found. The reaction pathways on the Pd/Ni model are all qualitatively similar to those on the pure Pd, but with important differences in the relative energies and barriers between the subsequent states along the profile, due to the specific paired and distorted structure on the Pd/Ni model. The lowest energy pathway is illustrated in Figure 2 for both the Pd and the Pd/Ni surfaces. For the first insertion of a hydrogen atom in the C−Pd bond, the ethylene molecule does not react preferably from the bridge site. First, it diffuses to a metastable precursor state, bound to a single Pd atom on a top site, while simultaneously a hydrogen atom migrates to an adjacent three-fold site. In this metastable state (24 kJ mol^{-1} less stable), the couple of adsorbates is prepared for reaction. Considering that the diffusion barriers (typically of the order of 20 kJ mol^{-1}) are small, the top and bridge adsorption sites are assumed to be in a chemical equilibrium. So, the most stable adsorption site (bridge) is not the reactive state, unlike what was found on Pd(111).[24] From this precursor state, the C−H bond formation occurs through the first transition state, TS1 (Figure 2), located 56 kJ mol^{-1} higher for Pd (42 kJ mol^{-1} for the Pd/Ni model). An ethyl molecule is formed in an eclipsed conformation, followed by a change to a staggered conformation. This fragment is slightly stabilized by coadsorption with an H atom on the pure Pd surface, but not on the Pd/Ni model deposit. This first hydrogenation step, from the initial bridge site to the most stable ethyl group, shows an important difference between the two surfaces, the nanostructured Pd/Ni deposit yielding a smaller activation energy (61 kJ mol^{-1} instead of 80 kJ mol^{-1}) and a reduced endothermic character (22 kJ mol^{-1} versus 27 kJ mol^{-1} for the reaction energy). Finally, the second hydrogenation step can take place, through the transition state TS2 (Figure 2), with an activation energy of 45 kJ mol^{-1} on Pd and 42 kJ mol^{-1} on the Pd/Ni model. The resulting staggered ethane molecule desorbs easily, in agreement with the weak interaction of alkanes with the Pd surfaces. The reaction from the ethyl group coadsorbed with a hydrogen atom to form the weakly adsorbed ethane is exothermic by 25 kJ mol^{-1} for Pd and by 29 kJ mol^{-1} on the Pd/Ni model.

In TS1, the transformation is more advanced toward the ethyl product on the Pd/Ni model deposit than on Pd, with a shorter C−H and a longer C−C bond (Figure 3). In addition, the modification of the Pd−Pd surface bonds is larger on the pure Pd surface, with H nearly inserted in a Pd−Pd bond, than on the Pd/Ni model. The stability of TS1 is a compromise between all bonds involved, resulting in a very similar total energy for the two systems. The reaction barrier difference is hence totally arising from the weakened stability of the initial adsorption state on the deposit. For the second reaction step, the geometry and energy position of TS2 are similar on both surfaces.

Electronic Properties

The difference in the behavior of the Pd and Pd/Ni systems toward the adsorption of ethylene may be related to the surface

(22) Filhol, J.-S. Reconstruction et activité catalytique induite par contrainte: une étude quantique des dépôts de Pd sur Ni(110). Thesis, École Normale Supérieure de Lyon, 2001.
(23) Filhol, J.-S.; Simon, D.; Sautet, P. *J. Phys. Chem. B* **2003**, *107*, 1604.
(24) Neurock, M.; Venkataraman, P. D.; van Santen, R. A. *J. Am. Chem. Soc.* **2000**, *122*, 1150.
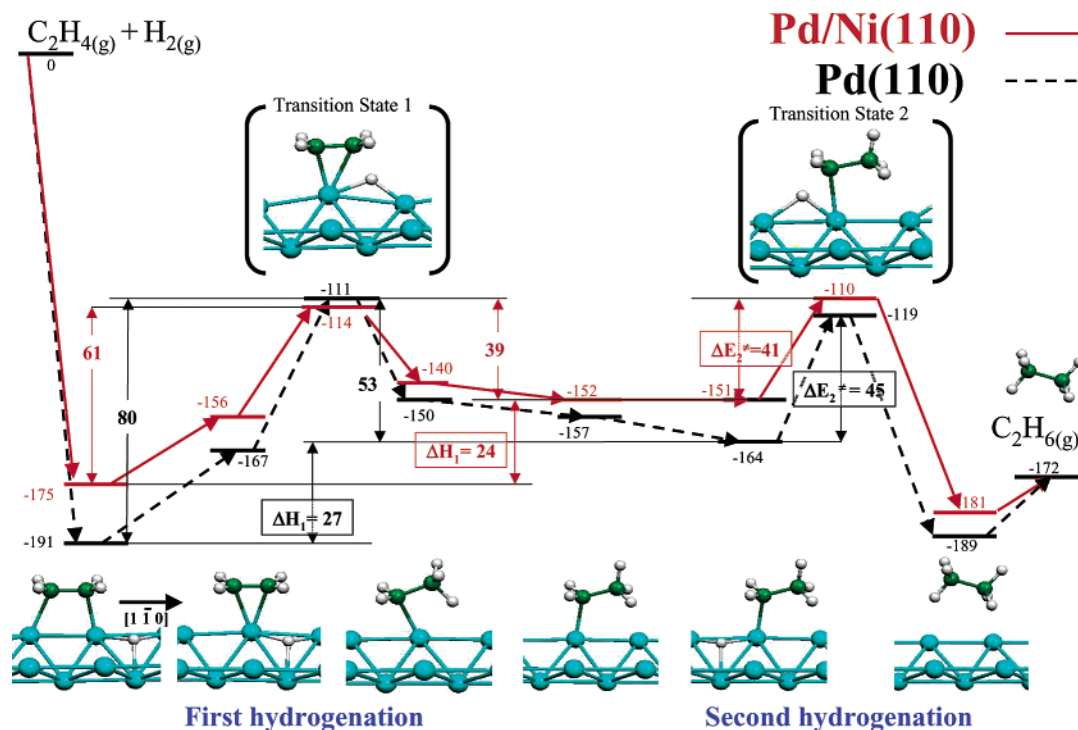
Figure 2. Reaction pathway of the two successive steps of hydrogenation of ethylene to ethane on a model Pd/Ni surface (full line) and a Pd(110) surface (dashed line). The energy values are given in kJ mol^{-1} and refer to the dihydrogen and ethylene molecules in the gaseous phase and the bare corresponding metal surface. In this figure, the zero-point energy corrections are not included in the energy positions of the intermediate and transition states.
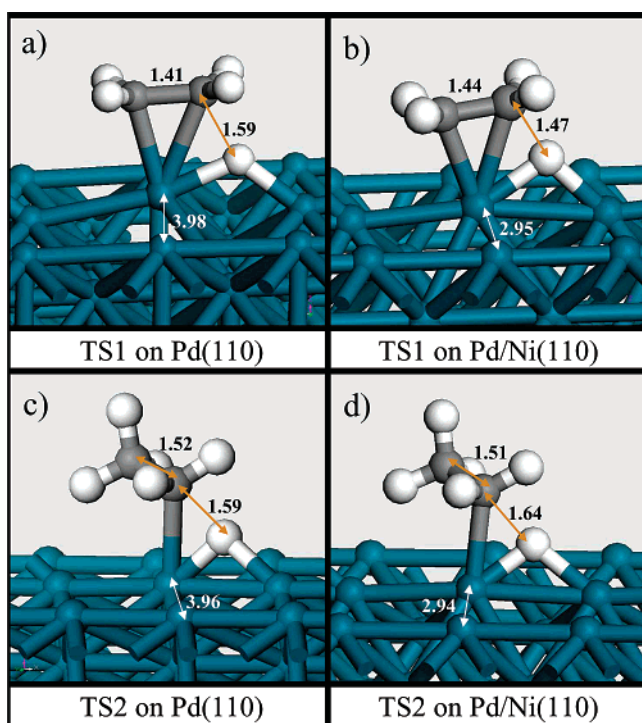
Figure 3. Structure of the different transition states on the hydrogenation pathway for the first hydrogenation step on (a) Pd(110) and (b) Pd/Ni-(110), and for the second hydrogenation step on (c) Pd and (d) Pd/Ni.

electronic structure. For the sake of clarity, the analysis of the adsorption is done for an ethylene molecule in the top geometry. In this case, the d_{xz} and d_{z^2} orbitals of the Pd atom overlap, respectively, with the π and π^* ethylene molecular orbitals, for topological reasons. Figure 4 presents a comparison of the electronic density of states of Pd and Pd/Ni, first in the case of a naked Pd surface, and then in the case of a surface with an
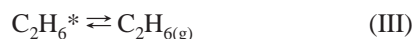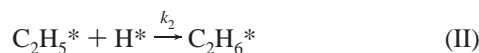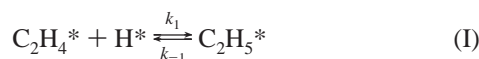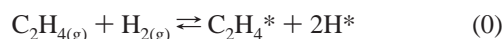
ethylene molecule adsorbed on a top site. When the Pd and Pd/Ni systems with the naked surface are compared, the d_{z^2} band (Figure 4a) shows an important modification close to the Fermi level, whereas the main features of the d_{xz} band (Figure 4b) remain nearly unchanged. The main peak of d_{z^2} is displaced toward a lower energy, getting away from the Fermi level. This behavior can be seen as a consequence of the pairing and buckling reconstruction. The buckling breaks the Pd–Pd bond between the surface and the third layer Pd atoms. The lack of d_{z^2} interaction between these two Pd atoms leads to a decrease of the width of the surface atom density of states, and consequently a loss of contribution close to the Fermi level. This induces a marked modification in the features of the d_{z^2} band, in the presence of an adsorbed ethylene molecule (Figure 4c). The interaction of d_{z^2} with a filled π orbital may be stabilizing, provided that antibonding states are efficiently pushed above the Fermi level. The weight of the energy contributions that are above the Fermi level is clearly larger in the Pd than in the Pd/Ni system. Consequently, these Pd–C antibonding levels are more efficiently emptied on Pd than on the Pd/Ni deposit. So, this behavior is associated with a less stabilized situation in the Pd/Ni case, as compared to the Pd system. The difference between Pd and Pd/Ni in the d_{xz} band, as the ethylene molecule is adsorbed (Figure 4d), is less noticeable. In both cases, the interaction with the π^* ethylene orbital yields emptied contributions far above the Fermi level and pushes down the peaks that were close to the Fermi level in the naked surface d_{xz} band (Figure 4b). This behavior is again stabilizing, but does not seem to differentiate the Pd and Pd/Ni systems. The lower adsorption energy of ethylene on the Pd/Ni surface then originates from the fact that the surface electronic structure is less suited to the interaction with the occupied ethylene π orbital.
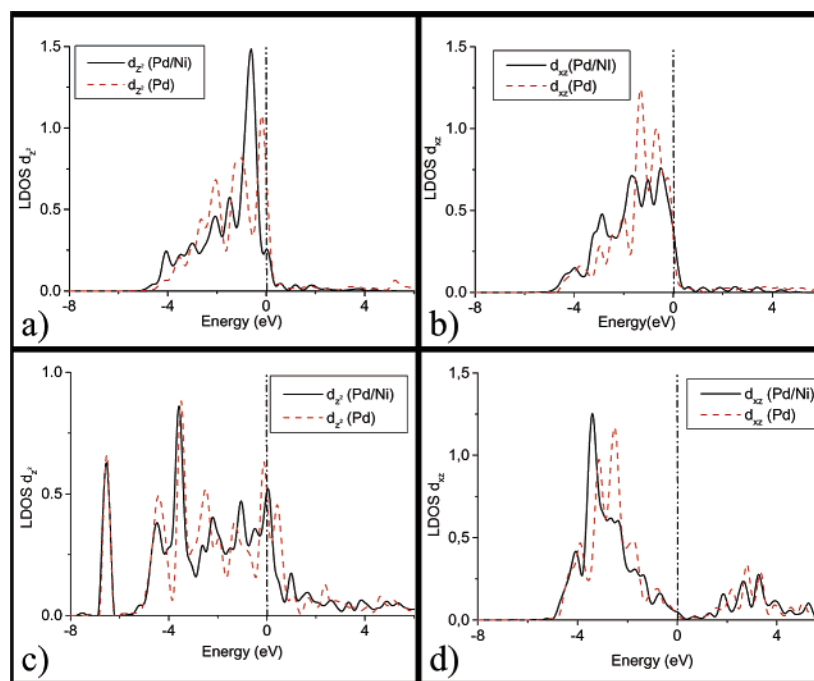
Figure 4. Electronic density of state for a surface Pd projected on (a) the d_{z^2} orbital and (b) the d_{xz} orbital for a bare Pd/Ni surface (straight line) and a bare Pd(110) surface (dashed line). Electronic density of state for a surface Pd projected on (c) the d_{z^2} orbital and (d) the d_{xz} orbital for a Pd/Ni surface (straight line) and a Pd(110) surface (dashed line) in the case of an adsorbed ethylene on a top site.

Discussion

From this first principle energy profile, a detailed kinetic model has been constructed to obtain a more detailed understanding of the compared hydrogenation reaction rates. The following mechanism results from the calculated pathways, where the adsorbed species are followed by a star:

$$C_2H_{4(g)} + H_{2(g)} \rightleftharpoons C_2H_4^* + 2H^* \qquad (0)$$

$$C_2H_4^* + H^* \underset{k_{-1}}{\overset{k_1}{\rightleftharpoons}} C_2H_5^* \qquad (I)$$

$$C_2H_5^* + H^* \overset{k_2}{\longrightarrow} C_2H_6^* \qquad (II)$$

$$C_2H_6^* \rightleftharpoons C_2H_{6(g)} \qquad (III)$$

The kinetics of the system has been simplified as follows. The adsorption reaction of ethylene and hydrogen is assumed to be very fast and corresponds to the global equilibrium (0). The first hydrogenation step (I) takes place from the most stable coadsorption state, through TS1, toward the most stable ethyl state. The second hydrogenation step (II) relates this ethyl state to an adsorbed ethane molecule, through TS2, the backward reaction being neglected due to a much higher activation barrier. The surface coverage of ethane can be neglected, because it has a very small desorption energy, and the desorption step is expected to be a nonactivated equilibrium (III).

The hydrogenation rate can be expressed as a function of the adsorbed species coverage θ, in the stationary surface limit:

$$r = -\frac{d[C_2H_{6(g)}]}{dt} = \frac{k_1 k_2}{k_{-1} + k_2\theta_H}\theta_{C_2H_4}\theta_H^2 \qquad (1)$$

The rate-limiting step is obtained from the comparison of k_{-1} and $k_2\theta_H$.

The ratio $k_2\theta_H/k_{-1}$ was evaluated from the exponential terms and activation barriers, assuming identical prefactors. The zero-point energy has been included from a vibrational calculation. This effect, equivalent on the two surfaces, is dominated by the contribution of the C–H stretch, and hence TS2, with one additional CH bond, is destabilized by 10 kJ mol^{-1} as compared to TS1. The ratio $k_2\theta_H/k_{-1}$ is calculated to 9×10^{-4} for the model Pd deposit on Ni and 0.11 for pure Pd, for the coverage $\theta_H = 0.25$ ML. Hence, as the first hydrogenation occurs as a quasi-equilibrium, with the constant $K_1 = k_1/k_{-1}$, the rates on the Pd and the Pd/Ni model surfaces can be written, respectively, as:

$$r_{Pd} = \frac{1}{1 + \dfrac{k_2^{Pd}\theta_H}{k_{-1}^{Pd}}} K_1^{Pd} k_2^{Pd} \theta_{C_2H_4}\theta_H^2 \qquad (2)$$

$$r_{Pd/Ni} = K_1^{Pd/Ni} k_2^{Pd/Ni} \theta_{C_2H_4}\theta_H^2 \qquad (3)$$

The values of the rates are then dominated by the energy behavior of K_1 and k_2:

$$r \approx e^{-\Delta H_1/k_B T} e^{-\Delta E_2^{\ddagger}/k_B T} \qquad (4)$$

where ΔH_1 is the enthalpy of the quasi-equilibrium (I), and $\Delta E_2^{\ddagger}$ is the activation energy of reaction II, both including the zero-point energy correction. Assuming that the entropy prefactors in K_1 and k_2 have the same value in Pd and the Pd/Ni model, the increase, ν, of catalytic activity on the strained deposit, as compared to the pure Pd surface, can be expressed as:

$$\nu = \frac{r_{Pd/Ni}}{r_{Pd}}$$

$$= e^{-[\Delta H_1(Pd/Ni) - \Delta H_1(Pd)]/k_B T} \; e^{-[\Delta E_2^{\ddagger}(Pd/Ni) - \Delta E_2^{\ddagger}(Pd)]/k_B T}$$

$$\times \left(1 + \frac{k_2^{Pd}}{k_{-1}^{Pd}} \theta_H\right) \quad (5)$$

The exponential terms are estimated, at 300 K, to be 7.5 and 3.3, respectively. The value of the expression $(1 + (k_2^{Pd}/k_{-1}^{Pd})\theta_H)$ is dependent on the H coverage (between 0 and 1 ML), but remains in the range $1-1.4$. As the energy positions of TS1 and TS2 are similar in both systems, the exponential terms in eq 5 are mainly related to the stability of the adsorbed intermediate species. Clearly, the increase of the rate in the Pd/Ni model system is linked to the fact that, on one hand, the adsorption energy of ethylene and, on the other hand, the coadsorption of the ethyl group with an H atom are both much lower on the Pd/Ni model than on pure Pd. ν is then estimated in the range $25-35$, in very good agreement with the experimental result, that shows an increase of the catalytic activity of 34.[9,10]

Conclusion

We have computed the various hydrogenation pathways from ethylene to ethane on both Pd(110) and 4 ML Pd/Ni(110) surfaces. The energetic behavior along the pathways allows one to model the kinetics and shows that the reaction rate on the 4 ML Pd/Ni(110) nanostructured surface is about 30 times larger than that on the Pd(110) surface, as found experimentally. This activity increase was associated with the strong destabilization of the ethylene adsorption on the Pd/Ni system, due to the peculiar surface nanostructure. Our computations demonstrate that the creation of nanostructured surfaces allows one to obtain an anisotropically stressed Pd surface. That layer exhibits unusual hybrid surface structures with the metallic atom in a completely different environment than any normal surface. This organization can lead to a striking enhancement of catalytic properties.

Using anisotropic stress to tailor structures with such a special atomic environment (perhaps also by other means than the epitaxial deposits) could then lead to an innovative way of designing new families of highly efficient catalysts.

JA038154C